Phase Transitions in the Early Universe

Electroweak and QCD Phase Transitions

Master Program of Theoretical Physics
Student Seminar in Cosmology

Author:
Doru STICLET

Supervisors:
Prof. Dr. Tomislav PROKOPEC
Drd. Maarten VAN DE MEENT

Contents

Abstract

The following report offers a review of two cosmological phase transitions: the electroweak and the QCD phase transitions in the early universe. The phase diagram of these transitions is discussed, as well as the nature of phases that appear in it. Theories about the eventual signature left by the phase transitions in the present universe are inventoried. Finally, the experimental search for the quark-gluon plasma is briefly examined.

Chapter 1

Introduction

As cosmology draws theoretical charts ever closer to the Big-Bang, it strives to validate them by finding footprints of universe's early creations. This report concern two of these: quantum chromodynamics (QCD) and electroweak phase transitions.

First goal is to simply understand the behavior of our theories at huge temperature scales, near Big-Bang. Then to see if experimental data can reach us out of these transitions.

The report is structured as an introduction to the study of QCD and electroweak phase transitions. Toy model theories are developed to show how different phase transition come out of breaking the symmetries of a particular Lagrangian (Ch. 2). It is also described why first order phase transitions are such a coveted prize in cosmology. If electroweak and QCD phase transitions would prove to be first order, then an explanation for matter-antimatter asymmetry would be at hand. Also detectable gravitational waves would be produced during nucleation of bubbles.

In the standard cosmological model, following inflation and after the *reheating* period, the universe enters a cooling process that continues today. At time $t \approx 10^{-12}$ s after Big-Bang, temperature drops to scales of $O(100\text{ GeV})$ and electroweak phase transition takes place. At this point electromagnetic and weak force differentiate through symmetry breaking of Minimal Standard Model (MSM) Lagrangian. The Higgs mechanism by which weak force becomes short range is reviewed (Sec. 3.1). The transitions phase diagram is described and evidence for electroweak theory to provide grounds for creating matter-antimatter asymmetry is considered (Sec 3.2).

At time $t \simeq 10^{-6}$ s after Big-Bang, the universe has reached a temperature of $O(100\text{ MeV})$. QCD phase transition takes place and quarks become confined into hadrons. This phase transition is susceptible to two interpretations: as deconfinement (Sec. 4.1-4.2) or as chiral symmetry breaking (Sec. 4.3). Using a phenomenological model to describe confinement we were able to find a critical temperature for this transition (Sec. 4.2) close to the more exact one obtained from lattice simulations (Sec. 4.1, 4.3). Then we switch from following closely T axis on the phase diagram-(T, μ) (were the evolution of universe's path lies) to relatively low temperatures and high densities (encountered in neutron stars), where we describe the

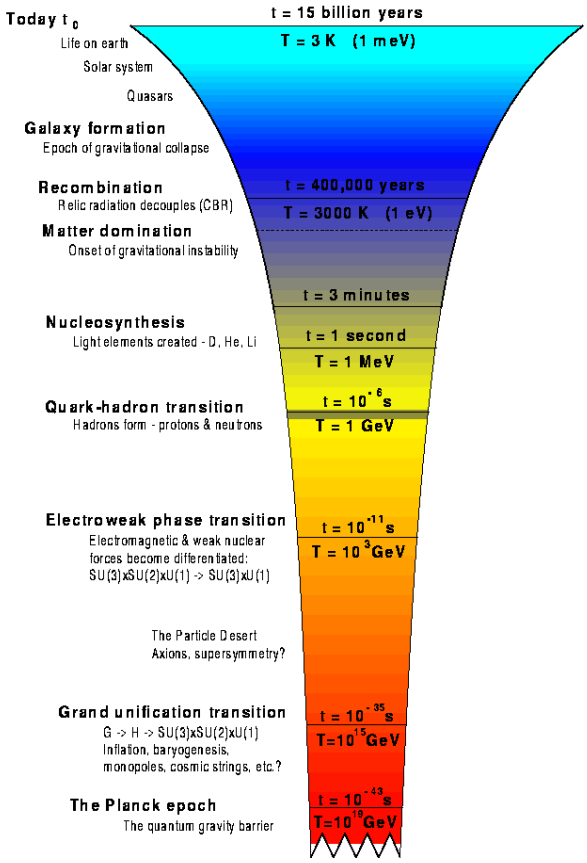

Figure 1.1: Thermal history of the universe in the standard cosmological model [1].

color-flavor locking (CFL) phase (Sec. 4.4). As data from cosmological QCD phase transition proves to be unattainable, efforts to recreate and detect in laboratories (especially RHIC) the high temperature quark-gluon plasma are illustrated (Sec. 4.5).

Chapter 2

Toy Models

In the following two sections we will study the way spontaneous symmetry breaking is related to thermal phase transitions. Taking two simple Lagrangians [2] we will obtain the effective potential as a function of the order parameter. The behavior of the effective potential dictates the type of the phase transition. These toy models also offer us the opportunity to describe features of the phase transitions that make them relevant in cosmology.

2.1 Crossover or Second Order Phase Transition

A crossover or a second order phase transition can be read from the following simple Lagrangian:

$$\mathcal{L} = \frac{1}{2}\partial_\mu\phi\partial^\mu\phi - V, \qquad V = \frac{\lambda}{4}(\phi^2 - v^2)^2, \tag{2.1}$$

where ϕ is a real scalar field, V is the potential, and λ, v are constants. This Lagrangian has the global symmetry $\phi \to -\phi$. The vacuum state of the system will spontaneously break the global symmetry of the Lagrangian. What we will show is that raising the temperature in the system, we will be able to induce a phase transition to a ground state wich obeys again the symmetry of (2.1).

The ground state of the system is determined by considering the minima of the potential. Thus taking $\frac{\partial V}{\partial \phi} = 0$, we obtain:

$$\lambda(\phi^3 - v^2\phi) = 0. \tag{2.2}$$

This shows that there are two non-zero solutions to Eq. (2.2), which describe the vacuum state of the system $\phi = \pm v$. That implies that the symmetry of the Lagrangian is broken by the system's choice of vacuum. Even at zero temperature there are quantum fluctuations of the field ϕ around one ground state [1]. But tunneling through the potential barrier to the other ground state of equal energy is exponentially suppressed. Switching on temperature will bring thermal fluctuations into our toy model. Considering that tunneling becomes significant only at

high temperatures means that we can ignore the more subtle quantum fluctuations in comparison with large thermal fluctuations. As temperature rises and thermal fluctuations grow, the field will begin to oscillate quickly between the minima of the system. These fluctuations will be so rapid that the average of the field over some large period of time will just give zero [1]. This is in sum the phenomenological description of the symmetry restoration process; where from a state were the field is trapped at a non-zero value we arrived by increasing temperature to a state symmetric under $\phi \to -\phi$, as the Lagrangian (2.1).

Factoring in temperature is done by decomposing the field $\phi(\mathbf{x})$ into a mean, homogenous part ϕ_0 plus a contribution from thermal fluctuations $\delta\phi(\mathbf{x})$. Considering here only Gaussian, symmetric thermal fluctuation means that averages over odd powers of $\delta\phi$ are zero. Using this decomposition of ϕ we return to Eq. (2.2), which now reads:

$$\lambda[\phi_0^3 + 3\phi_0^2\delta\phi + 3\phi_0\delta\phi^2 + \delta\phi^3 - v^2(\phi_0 + \delta\phi)] = 0. \tag{2.3}$$

Averaging over the fluctuations and eliminating averages of odd powers of $\delta\phi$ gives:

$$\lambda(\phi_0^3 + 3\langle\delta\phi^2\rangle\phi_0 - v^2\phi_0) = 0. \tag{2.4}$$

The value of the average $\langle\delta\phi^2\rangle$ can be found by Fourier decomposing $\delta\phi$ and quantizing the result, such that the Fourier coefficients will become annihilation and creation operators with familiar commutations relations between them [3]. Taking the vacuum expectation value of the product of two fluctuation fields $\delta\phi$ gives [3]:

$$\langle\delta\phi^2\rangle = \int \frac{d^3\mathbf{p}}{(2\pi)^3}\frac{1}{\omega}\left(\frac{1}{2} + n_{\mathbf{p}}\right) \qquad \text{with} \quad \omega = \sqrt{\mathbf{p}^2 + m^2}, \tag{2.5}$$

where $n_{\mathbf{p}}$ is the occupation number and m is the mass of the field given by $m^2 = \partial_\phi^2 V|_{\phi_0=\pm v} = 2\lambda v^2$. Taking finite temperature into account implies substituting the occupation number $n_{\mathbf{p}}$ with the Bose-Einstein distribution function. The $1/2$ term in Eq. (2.5) is divergent and represents the infinite contribution from the zero-temperature. We will disregard this term as it is absorbed during renormalization in the couplings of the theory. Then, considering only the thermal contribution, we obtain:

$$\langle\delta\phi^2\rangle = \int \frac{d^3\mathbf{p}}{(2\pi)^3}\frac{1}{\omega}\frac{1}{e^{\beta\omega} - 1}. \tag{2.6}$$

Let us solve this integral by first going to polar coordinates and then changing the integration variable $p \to \omega$. From now on we will denote the integral (2.6) by I. Then:

$$I(m) = \frac{1}{2\pi^2}\int_m^\infty d\omega \frac{\sqrt{\omega^2 - m^2}}{e^{\omega/T} - 1}. \tag{2.7}$$

We wish to work in the high temperature limit, so it will be helpful to write the parameters in our problem divided by T:

$$x = \frac{\omega}{T}, \qquad y = \frac{m}{T}. \tag{2.8}$$

Then we rewrite the integral I:

$$\begin{aligned} I(y) &= \frac{T^2}{2\pi^2}\int_y^\infty dx \frac{\sqrt{x^2-y^2}}{e^x-1} \\ &= \frac{T^2}{2\pi^2}\sum_{n=1}^\infty \int_y^\infty dx\sqrt{x^2-y^2}e^{-nx}. \end{aligned} \tag{2.9}$$

In order to solve this integral, we can first solve the easier one:

$$\begin{aligned} \frac{\partial I(y)}{\partial y} &= \frac{-yT^2}{2\pi^2}\int_y^\infty \frac{e^{-nx}}{\sqrt{x^2-y^2}} \\ &= \frac{-yT^2}{2\pi^2}\sum_{n=1}^\infty K_0(ny), \end{aligned} \tag{2.10}$$

where K_0 is a modified Bessel function with a integral expression given above. We can perform the sum over K_0 in the high temperature limit ($y \ll 1$) and maintain only the leading order [3, 4].

$$\frac{\partial I(y)}{\partial y} = -\frac{yT^2}{2\pi^2}\left(\frac{\pi}{2y} + O(\ln y)\right) \tag{2.11}$$

Then to the leading order:

$$\begin{aligned} I(y) &= \int_0^y dy' \frac{\partial I(y')}{\partial y'} + I(0) \\ &= -\frac{yT^2}{4\pi} + \frac{T^2}{2\pi^2}\sum_{n=1}^\infty \int_0^\infty dx x e^{-nx} \\ &= -\frac{yT^2}{4\pi} + \frac{T^2}{2\pi^2}\sum_{n=1}\frac{1}{n^2} \\ &= -\frac{yT^2}{4\pi} + \frac{T^2}{12}, \end{aligned} \tag{2.12}$$

where the last sum is the already known $\zeta(2) = \frac{\pi^2}{6}$.

In conclusion, the thermal contribution to the propagator $\langle\delta\phi^2\rangle$ in leading terms in temperature T is:

$$\langle\delta\phi^2\rangle \simeq \frac{T^2}{12} - \frac{mT}{4\pi}. \tag{2.13}$$

For the present purpose, we can use a cruder approximation by taking only the leading term $O(T^2)$ in Eq. (2.4). It will now read:

$$\lambda\left(\phi_0^2 + \frac{T^2}{4} - v^2\right)\phi_0 = 0 \tag{2.14}$$

Integrating this equation, we obtain an effective potential which describes how the homogenous field ϕ_0 is influenced by temperature:

$$V_{eff}(\phi_0) = \lambda \left[\frac{\phi_0^4}{4} + \frac{\phi_0^2}{2} \left(\frac{T^2}{4} - v^2 \right) \right] \tag{2.15}$$

This basically allows you to construct a theory of the field ϕ_0, from which you can derive the evolution of ϕ_0. For our previous theory (2.1), it means that we found how the expectation value of field ϕ behaves under temperature effects.

From Eq. (2.14) we can obtain a critical temperature T_c in our system. If $T > T_c = 2v$, Eq. (2.14) has only $\phi_0 = 0$ solution, while for $T < T_c$, ϕ_0 has two non-zero minima. This implies that we have a phase transition at T_c such that the field ϕ developes an expectation value ϕ_0 under a certain temperature $T_c = 2v$. In conclusion, we found out that the symmetry of the Lagrangian is broken by the ground state below T_c, where ϕ_0 has non-zero value. Above T_c the symmetry is restored and $\phi_0 = 0$. This general feature will be seen again in the treatment of electroweak and QCD phase transitions.

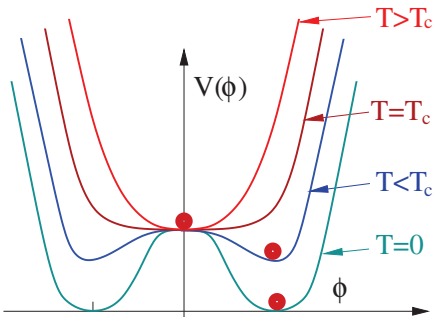

Figure 2.1: Crossover or second order phase transition. The figure should be read as $V_{eff}(\phi_0)$ [1].

Drawing the graph of the effective potential $V_{eff}(\phi_0)$ at different temperatures, we recognize immediately a second phase transition or a crossover. Mean field ϕ_0 plays the role of the order parameter in this transition. We can read the evolution on the mean field ϕ_0 with the decreasing temperature. As we can see the field ϕ develops an expectation value as temperature drops below T_c. The field rolls during this process from fluctuating around zero value to some non-zero value in a smooth manner. This underlines the following important feature of crossovers (or second order phase transitions): they are continuous in the order parameter. During such transitions we are constantly at thermal equilibrium. This means that the system looses the memory of the initial state from which it begun. Thus, we don't expect remnants at lower temperatures ($T < T_c$) from the unbroken phase, such as bubbles of $\phi_0 = 0$, domain walls, etc. This makes second order phase transitions (and crossovers) not so interesting from the point of view of cosmology. If the electroweak and QCD phase transitions are proven to be of this kind, we do not expect to get

astrophysical data about them. Also the hypothesis that matter-antimatter asymmetry is explained by the electroweak phase transition would become problematic.

2.2 First Order Phase Transition

Let us turn our attention to a more complicated Lagrangian from which we can read a first order phase transition [2]:

$$\mathcal{L} = \frac{1}{2} D_\mu \phi^* D^\mu \phi - \frac{\lambda}{4}(\phi^* \phi - v^2)^2 - \frac{1}{4} F_{\mu\nu} F^{\mu\nu}. \tag{2.16}$$

where the covariant derivative is defined $D_\mu = \partial_\mu + igA_\mu$ and the field strength tensor $F_{\mu\nu} = \partial_\mu A_\nu - \partial_\nu A_\mu$. This Lagrangian can be said to be obtained from the previous Lagrangian (2.1), when we demand invariance of (2.1) under local phase transformation:

$$\phi \to e^{i\theta(x)} \phi \tag{2.17}$$

This is realized by introducing a complex field ϕ. To solve the invariance breaking by the derivative of (2.1), we turn the regular derivative into a covariant derivative and define in it a vector field A_μ with a transformation law:

$$A_\mu \to A_\mu - \frac{1}{g} \partial_\mu \theta, \tag{2.18}$$

where g is the charge of the field A_μ. In this way the Lagrangian becomes invariant under (2.17).

In order to make calculations more transparent, we decompose the complex field ϕ into two real fields $\phi = \phi_1 + i\phi_2$. Mirroring the procedure displayed in the previous section, we will decompose the latter fields in some mean, homogenous value and a part dependent on thermal fluctuations. Because the system is phase rotation invariant, ϕ can be transformed such that ϕ_1 will have a real expectation value ϕ_0, while ϕ_2 becomes a pure fluctuation:

$$\phi_1 = \phi_0 + \delta\phi_1, \qquad \phi_2 = \delta\phi_2. \tag{2.19}$$

To find the ground state of the system, we must minimize the potential in (2.16) with respect to ϕ_1:

$$\lambda(\phi_1^2 + \phi_2^2 - v^2)\phi_1 + g^2 A^2 \phi_1 = 0. \tag{2.20}$$

Under our choice of the real fields and as long as fluctuations are taken to be Gaussian, ϕ_2 is not so interesting, because it cannot break the symmetry of the Lagrangian. Introducing the above field expressions in Eq. (2.19) and averaging over the fluctuations gives:

$$\lambda \left[\phi_0^2 + 3\left\langle \delta\phi_1^2 \right\rangle + \left\langle \delta\phi_2^2 \right\rangle + \frac{g^2}{\lambda} \left\langle A_\mu A^\mu \right\rangle - v^2 \right] \phi_0 = 0 \tag{2.21}$$

Note also that A_μ is a massive gauge boson not unlike the photon met in massive QED. Its mass m is seen by expanding the covariant derivatives in (2.16). The presence of ϕ_0 gives it a mass $m^2 = g^2\phi_0^2$.

A_μ has three degrees of freedom such that it has three times the *thermal contribution* (only this contribution is considered here) of the scalar boson field $\delta\phi$ from Eq. (2.6):

$$\langle A_\mu A^\mu \rangle \simeq \frac{T^2}{4} - \frac{3mT}{4\pi} \tag{2.22}$$

Using also the expansion of the other $\delta\phi_{1,2}$ fields to the leading order in T, we obtain from Eq. (2.21):

$$\lambda\left[\phi_0^2 - \frac{3g^3T\phi_0}{4\pi\lambda} + \left(\frac{1}{3} + \frac{g^2}{4\lambda}\right)T^2 - v^2\right]\phi_0 = 0 \tag{2.23}$$

Integrating this equation we find the effective potential $V_{eff}(\phi_0)$:

$$V_{eff}(\phi_0) = \frac{1}{2}\left[\left(\frac{\lambda}{3} + \frac{g^2}{4}\right)T^2 - \lambda v^2\right]\phi_0^2 - \frac{g^3T}{4\pi}\phi_0^3 + \frac{\lambda}{4}\phi_0^4 \tag{2.24}$$

From (2.24) we can read the expectation value behavior of ϕ_1 as a function of temperature. Its behavior is illustrated in Fig. 2.2.

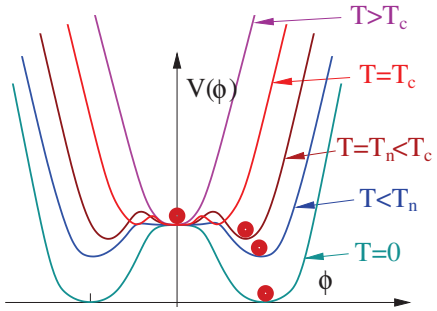

Figure 2.2: First order phase transition. The figure should be read as $V_{eff}(\phi_0)$ [1].

Presence of the ϕ_0^3 term in V_{eff} signals a first order phase transition. The cubic term translates in Fig. 2.24 as two symmetric local maxima. As temperature drops, maxima develop as potential barriers that keep field's expectation value trapped in the origin. At a critical temperature T_c all three minima of the potential become equal. This condition determines:

$$T_c = \sqrt{\frac{12\lambda v^2}{4\lambda + 3g^3 - (3g^6)(2\pi^2\lambda)}} \tag{2.25}$$

As the temperature drops further, V_{eff} assumes smaller value at non-zero value minima, than at $\phi_0 = 0$. The field remains trapped in the origin, but it would be energetically favorable for it to sit in the true vacuum provided by secondary minima.

Under a nucleation temperature T_n, the potential barrier becomes smaller and the probability for the field to tunnel to the true vacuum becomes larger then expansion rate of the universe. Then nucleating bubbles, instead of being suppressed, begin to expand in the background of the symmetric state of false vacuum. Eventually, the field rolls in the true vacuum and gains a non-zero expectation value. It is now in a ground state that breaks the symmetry of the Lagrangian (2.1). In short, symmetry breaking of the phase rotation lead to developing a non-zero expectation value for ϕ_1, and by this process the gauge field A_μ gains mass $m^2 = g^2\phi_0^2$.

First order phase transitions are relevant for cosmology because it exhibits processes out of thermal equilibrium at the bubble walls. During transition space is no longer isotropic and homogenous and time reversal symmetry is broken. Pressure difference in the two phases drives the expansion of the bubbles. Bubble wall acceleration quickly leads to relativistic speeds and a large kinetic energy is associated to them. Then bubble nucleation can be a violent event like boiling water. At electroweak scales bubbles expand in space, crashing into each other and releasing energy as particles, but also as gravitational waves. These gravitational waves could in principle be detected experiments. A different consequence of cosmological first order transitions could be the formation of domain walls. Different, but energetically degenerate, vacua can be chosen in separate regions of space. As these regions expand, domain walls can form at their meeting point. Domain walls would act as a potential barrier between the different vacua and thus have a positive energy associated to them. If their length stretches large portions of space, then their total energy would be high enough for them to be detected. In conclusion, remnants can be expected from first order phase transitions and hope was that QCD or electroweak phase transition would have produced them. Detection of these remnants would offer us a valuable sneak peek into a yet unseen past and would directly put to test our theories.

Chapter 3

Electroweak Phase Transition

3.1 Reviewing the Higgs Mechanism

A description of what electroweak phase transition means from the point of view of gauge symmetries is condensed in the following expression:

$$SU(3)_c \otimes SU(2)_L \otimes U(1)_Y \rightarrow SU(3)_c \otimes U(1)_{EM} \tag{3.1}$$

Physically, it describes the moment in our universe evolution when electric and weak forces differentiate. At temperature scales above ~ 100 GeV, MSM Lagrangian exhibits the gauge symmetry: $SU(3)_c \otimes SU(2)_L \otimes U(1)_Y$. $SU(3)_c$ refers to the color symmetry and plays no role in our rendition of the electroweak phase transition. From now on it will be neglected. $SU(2)_L$ is the symmetry group for transformations of the left fermions and it is associated to gauge fields $W_\mu^\pm$ and Z_μ. $U(1)_Y$ is the symmetry group for simple local phase transformations of the MSM Lagrangian and has associated the gauge field B_μ. A Lagrangian obeying the above symmetries contains only massless gauge fields. But if the weak force mediators are massless, the force itself displays long range behavior (exactly as massless photons make electromagnetic forces long range). But this is not the situation encountered in nature. The challenge was then to create mass for W and Z bosons. Simply including mass terms for the gauge fields into the Lagrangian breaks its gauge invariance.

The solution was eventually found by invoking the idea of *spontaneous symmetry breaking*. What it says is that the ground state of the system does not have to obey the symmetries of the Lagrangian. A typical Lagrangian predicts a manifold of equivalent ground states, but only one might be chosen by the system. By Goldstone theorem, this symmetry breaking leads to creation of massless bosons. The final act in the story comes with Higgs mechanism, by which massless gauge bosons *absorb* the degrees of freedom of the Goldstone would-be bosons to become massive.

In our case, we must assume that at the electroweak phase transition's critical temperature spontaneously symmetry breaking and Higgs mechanism take place. In order to understand how temperature influences the electroweak phase transition, a brief review of how Higgs mechanism works is salutary.

Here we will introduce one of the simplest models for the Higgs mechanism [5, 6]. First step is to introduce in the theory a scalar doublet of the form:

$$H = \frac{1}{\sqrt{2}} \begin{pmatrix} 0 \\ \rho \end{pmatrix} e^{i\phi^{(a)} t_a^{(F)}}, \tag{3.2}$$

where $t_a^{(F)} = \frac{1}{2}\tau_a$, while $\phi^{(a)}$ and ρ are scalar fields ($a = 1, 2, 3$). If we add to the MSM Lagrangian the following Higgs Lagrangian, the gauge invariance is manifestly maintained:

$$\mathcal{L}_{Higgs} = -(D_\mu H)^\dagger D^\mu H - \mu^2 H^\dagger H - \lambda (H^\dagger H)^2, \tag{3.3}$$

where

$$D_\mu = \partial_\mu - igW_\mu^a t_a^{(F)} - ig' B_\mu Y, \tag{3.4}$$

and $Y = \text{diag}(1, 1)$ is the generator of hypercharge group $U(1)_Y$ in flavor space, and g, g' are coupling constants.

In unitary gauge, H assumes the simpler form $H = \frac{1}{\sqrt{2}} \left(\begin{smallmatrix} 0 \\ \rho \end{smallmatrix}\right)$. At this point we transformed away the $\phi^{(a)}$ fields, which would have been the Goldstone bosons. Choosing in $\mathcal{L}_{Higgs}$, the parameter μ such that $\mu^2 < 0$, we find the minima of the Higgs potential at:

$$\langle H \rangle = \frac{1}{\sqrt{2}} \begin{pmatrix} 0 \\ v \end{pmatrix}, \qquad v = \sqrt{\frac{-\mu^2}{\lambda}}, \tag{3.5}$$

where $v \simeq 246$ GeV is the vacuum expectation value.

The choice of μ was such that $\langle H \rangle$ breaks the symmetries of the Lagrangian. Now generators of the gauge symmetry groups applied on this ground state no longer annihilate it. But we can still find just one combination of generators that annihilate it:

$$t_3 + Y/2 = Q, \tag{3.6}$$

where Q is the generator of $U(1)_Q$ gauge symmetry group. This turns out to be exactly the gauge symmetry group of electromagnetism. Then the symmetry breaking is encapsulated in:

$$SU(2)_L \otimes U(1)_Y \to U(1)_{EM}. \tag{3.7}$$

Mirroring the work done in the previous chapter we could write:

$$H = \langle H \rangle + \delta H = \frac{1}{\sqrt{2}} \begin{pmatrix} 0 \\ v + h \end{pmatrix}, \tag{3.8}$$

where $h(x)$ is the Higgs boson and v is the vacuum expectation value. Expanding the covariant derivatives in (3.3), one obtains mass terms for W and Z bosons:

$$\begin{aligned} m_Z^2 &= \frac{(g^2 + g'^2)v^2}{4} = 91.1887 \pm 0.0044 \text{ GeV}, \\ m_{W^\pm}^2 &= \frac{g^2 v^2}{4} = 80.412 \pm 0.043 \text{ GeV} \end{aligned} \tag{3.9}$$

Now we can understand the importance of the non-zero expectation value v. Without symmetry breaking, $v = 0$ and the weak bosons lose their mass. Finally we note that in the same calculation in which we got m_Z and m_W, the Higgs boson acquires mass. Also the quarks get mass by their coupling to the H doublet within the Yukawa sector of the MSM Lagrangian.

3.2 Electroweak Phase Transition

To determine the order of electroweak phase transition, the behavior of the effective potential must be analyzed. The effective potential $V_{eff}(\langle H \rangle)$ contains information about vacuum's expectation value dependence on temperature. Similarly to the toy models developed in Ch. 2, it is found that at high temperature, the vacuum expectation value is zero, the ground state obeys the symmetries of the Lagrangian and weak gauge boson masses are zero. At a critical temperature $T_c \sim m_h/g$ (m_h is Higgs mass and g, weak coupling constant) [7], we enter the broken phase where particles gain mass through Higgs mechanism.

The best methods employed to construct the effective potential fall into two categories: perturbative calculations or lattice simulations. We will begin by reviewing the first option. Unlike QCD, perturbative methods are more successful here because the nature of the Higgs mechanism is itself perturbative. The main line of attacking the problem involves developing finite temperature effective field theories.

The first step in obtaining V_{eff} is to expand relevant field into a mean, homogenous part and one dependent on thermal fluctuations. Then this expression of the field is inserted into the action S. For a field $\phi(x) = \phi_0 + \delta\phi(x)$, the path integral will read [1]:

$$Z = \int \mathcal{D}\phi_0 \mathcal{D}\delta\phi \exp(iS_0[\phi] + S_2[\phi_0, \delta\phi] + S_{int}[\phi_0, \delta\phi]), \tag{3.10}$$

where $S_2[\phi_0, \delta\phi]$ contain terms up to quadratic in $\delta\phi$ and $S_{int}[\phi_0, \delta\phi]$, higher order terms in fluctuations. Then a Taylor expansion of terms containing $\delta\phi$ is carried out to the desired order. In electroweak theory it was possible to go to 2-loop order in perturbations [1]. After this, $\delta\phi$ is integrated out, to obtain an effective action S_{eff} dependent only on the mean expectation value of ϕ. Then V_{eff} can be extracted from S_{eff} and analyzed to yield the type of the phase transition, critical temperature, etc.

Perturbative techniques present important limitations in electroweak theory. If the phase transition is a crossover or weakly first order, the relevant fields develop long range correlations that cannot be addressed within perturbation theory [1]. Also, each loop in the perturbative expansion bring a contribution of the order g^2T/m. At phase transition light excitation with mass $m \lesssim g^2T$ appear, such that an infrared divergences develop in the theory, and perturbation expansion breaks down [7].

Better results come from lattice simulations. In order to make the problem more computationally tractable, dimensional reduction is applied to the original theory. From a $4d$ theory at finite temperature, a $3d$ $SU(3) \otimes U(1)+$ Higgs theory, effective theory with the following Lagrangian is obtained [8]:

$$\mathcal{L} = \frac{1}{4}F_{ij}^a F_{ij}^a + \frac{1}{4}B_{ij}B_{ij} + (D_i H)^\dagger D_i H + m_3^2 H^\dagger H + \lambda_3 (H^\dagger H)^2, \tag{3.11}$$

where $F_{ij}^a = \partial_i A_j^a - \partial_j A_i^a - g_3 \epsilon^{abc} A_i^b A_j^c$, $B_{ij} = \partial_i B_j - \partial_j B_i$, $D_i = \partial_i + i g_3 \sigma_a A_i^a/2 + i g_3' B_i/2$ and the couplings $g_3, g_3', m_3, \lambda_3$ are functions dependent on temperature and $4d$ theory's couplings. Numerical treatment of $3d$ effective theory have yielded that within MSN, the transition is first order up to a Higgs mass $m_h = 72 \pm 2$ GeV [9]. But LEP measurements have excluded $m_h < 115$ GeV. In conclusion, electroweak phase transition is most likely a crossover. That means no remnants are to be expected from this transition.

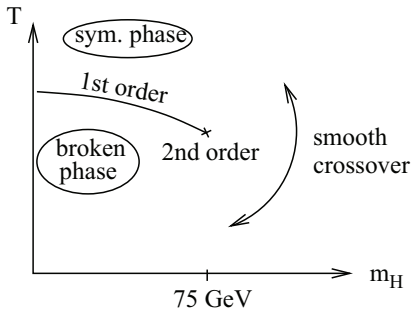

Figure 3.1: Electroweak crossover phase transition in MSM [10].

These conclusions hold only within MSM. The electroweak phase transition in MSSM (Minimal Supersymmetric Standard Model) was also thoroughly analyzed through lattice simulation [11] and it was proved that strong first order transition occurs at higher values of $m_h \sim 95$ GeV. Other calculations showed that for $m_h \simeq 116$ GeV a first order transition still takes place [12]. Vindication of supersymmetric models at LHC could thus bring electroweak theory in a position to explain one of the biggest problems in cosmology: matter-antimatter asymmetry.

We will end the chapter with a short description of how a first order electroweak phase transition could solve this problem. During bubble nucleation, thermal equilibrium is broken inside bubble walls. This gives rise to charges that diffuse outside the bubbles in the symmetric phase and CP violating currents form [13]. There, due to the currents and unsuppressed sphaleron transition, it becomes energetically favorable for the system to gain a non-zero baryon number. As bubble walls expand, baryon asymmetries are absorbed into the broken phase [13]. Thus an initial small excess of mater over antimatter can lead during universe expansion to matter domination at matter-radiation equality $z_{eq} = 3230 \pm 210$ [1].

Chapter 4

QCD Phase Transition

4.1 QCD Phase Transition as Deconfinement

After the electroweak phase transition, the universe cools further more, until temperatures reach scales $O(100\text{ MeV})$. A new phase transition is predicted there: the QCD phase transition.

At asymptotic high temperatures, the QCD coupling constant $g_s \to 0$, such that quarks behave like free particles. They are said to form a quark-gluon plasma (QGP). Although the running of QCD coupling constant indicates an increase in g_s as temperature drops, at sufficient high temperatures ($T \sim O(1\text{ GeV})$), perturbative treatment of QGP can be considered exact. Analytical perturbative calculations encounter problems at scales of interest $O(100\text{ MeV})$, when we can no longer assume $g_s \ll 1$ [3]. With increase in strength of the strong force, the QGP plasma of weakly interactive quarks gets replaced with the more familiar hadronic phase in which quark appear bound in baryons and mesons. This phenomena is called *confinement* and is the perspective on the QCD phase transition explored in this section.

Because baryons and mesons are color neutral, while (colored) quarks are encountered only at small scales, inside the hadrons, the confinement phase transition can be cast into symmetry breaking language as:

$$SU(3)_c \otimes U(1)_{EM} \to U(1)_{EM}, \tag{4.1}$$

where color symmetry group is broken to electromagnetism's symmetry group. Note that this is only a matter of speaking, as direct breaking of $SU(3)_c$ would lead to massive gluons. Here (4.1) only suggests quark confinement.

The most important questions raised in the study of the QCD phase transitions are: What is the type of this transition? What is its critical temperature? How does one determines quantitatively the phase diagram?

Perturbative techniques in determining characteristics of hadronic and QGP phases at temperatures $T \sim O(100\text{ MeV})$ fail, as coupling constant g_s diverges at that order. The best avenues for exploring the phase transition either involve phe-

nomenological models like the *MIT bag model* or lattice QCD simulations. The most precise proved to be the latter ones.

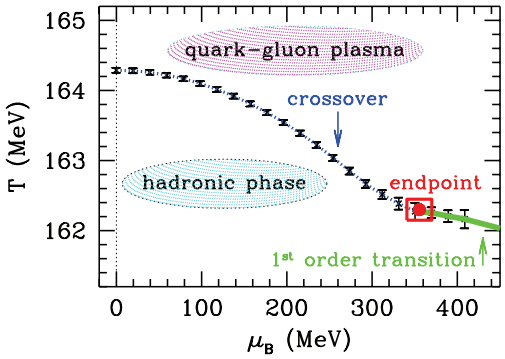

Figure 4.1: QCD phase diagram obtained through lattice simulation. Endpoint E determined by $T_E = 162 \pm 2$ MeV and $\mu_E = 360 \pm 40$ MeV. Data taken from [14].

Monte Carlo simulations were able to reproduce with good accuracy a large part of the (μ, T)-phase diagram, up to chemical potential $O(400\ \text{MeV})$ ($\sim$ neutron star densities) where they break down. As it can be see from Fig. 4.1, lattice simulations revealed that cosmological QCD phase transition was most probably a crossover [14]. The universe evolves at small baryon chemical potential μ and high temperature T, such that its path on the (μ, T)-diagram takes it to the left from the endpoint E. The endpoint marks a second order phase transition as limit case of a first order phase transition and was determined accurately (see, Fig. 4.1). If QCD phase transition is a crossover, then most likely there are no remnants of it in today's universe.

Critical temperature T_c was determined during the same simulations:

$$T_c = 164 \pm 2\ \text{MeV} \tag{4.2}$$

At this point we leave lattice calculations to develop a simple phenomenological model that enables us to determine deconfinement critical temperature close to the lattice value (4.2).

4.2 The *Bag Model* and the QCD Phase Transition

If we adopt the point of viewing the QCD phase transition as (de)confinement, we can produce a simple calculation of its critical temperature T_c. This can be done using a simplified version of the *bag model* [15].

Our *bag model* treats hadrons like little bubbles or bags in which the quarks are to be treated as free particles. This models the asymptotic freedom of QCD. Quarks are confined into hadrons and cannot break out of the bags. To achieve confinement, the model assumes a bag constant B for the region of free quarks. This is done to

simulate a pressure exerted by the bulk vacuum, keeping quarks confined. If we consider the hadrons approximately spherical, with a radius R, the energy associated with the existence of B is just $\frac{4\pi}{3}R^3B$. There is also a kinetic energy associated with the free quarks which can be determined from the uncertainty principle to be $\sim 1/R$. Adding these contribution to the hadron energy E_H results in:

$$E_H = \frac{4\pi}{3}R^3B + \frac{C}{R}, \tag{4.3}$$

where C is a constant determined by minimizing E_H with respect to R:

$$C = 4\pi BR^4. \tag{4.4}$$

Eliminating C in E_H and equating energy and hadron mass M, we find:

$$M = \frac{16\pi}{3}R^3B. \tag{4.5}$$

To determine an average value for the bag constant B, we take the average hadron mass $M \simeq 1$GeV. As a result: $B^{1/4} \simeq 200$ MeV. We also note that the inward, confining pressure is directly proportional to B: $P = -\partial_V E_H = -B + C/4\pi R^4$.

To find the critical temperature T_c of the phase transition between confined and deconfined phases, we will introduce a series of simplifying assumptions. Firstly, at transition temperature, only the lightest quarks u and d are considered. Because of the high temperature, it is justifiable to work in the ultrarelativistic limit, where the mass of the relevant quarks and antiquarks is approximately zero. In the hadron phase, near T_c, the dominant hadrons are the lightest mesons, the pions $\pi^{\pm}$ and π^0. The final assumption consists in taking baryon chemical potential $\mu = 0$.

This assumptions allows one to consider both hadrons in the broken phase and QGP in the symmetric phase as ultrarelativistic fluids, such that an expression for their pressure is easily computed. To determine the effective number of relativistic degrees of freedom, we consider for hadronic fluid pressure, P_H, the three charge state of the pion and the negative pressure due to the presence of the bag constant B and for QGP pressure, P_{QGP}, we take into account 8 gluons with 2 helicity states, 2 quarks, 2 antiquarks, each with 2 helicity states and 3 colors, and the usual fermionic statistic factor $7/8$ [1]. The result reads:

$$\begin{aligned} P_H &= 3 \times \frac{\pi^2 T^4}{90} - B, \\ P_{QGP} &= \left(\underbrace{2 \times 2 \times 2 \times 3 \times \frac{7}{8}}_{quarks} + \underbrace{2 \times 8}_{gluons} \right) \frac{\pi^2 T^4}{90}. \end{aligned} \tag{4.6}$$

At the critical temperature T_c we can the invoke equality of pressure in the two phases, such that from (4.6) and $B^{1/4} \simeq 200$ MeV we obtain:

$$T_c = \left(\frac{45B}{17\pi^2} \right)^{1/4} \simeq 144 \text{ MeV}. \tag{4.7}$$

In conclusion, we found that at zero chemical potential a first order phase transition is expected between hadronic and QGP phases. As we have seen from the phase diagram, this findings are invalidated once the mass of the quarks is switched on. The tendency observed is that the first transition line retracts to higher μ, such that at $\mu = 0$ we only encounter a crossover. On the plus side, the critical temperature obtained here is certainly close to the value predicted by lattice simulations $T_c \simeq 164$ MeV.

The last observations concern general limitations of the *bag model*. This model was constructed on phenomenological grounds without being derived from the QCD Lagrangian. Although it helps organizing our physical intuition about the processes occurring at T_c, it fails in delivering good results at high μ [15]. Also by considering from the beginning a difference of phases at the hadron bag limit, it has a built in bias towards predicting a first order phase transition. In any respect, numerical results obtained in lattice QCD remain superior to its predictions.

4.3 QCD Phase Transition as Chiral Symmetry Breaking

Deconfinement is not the only perspective to look at the QCD phase transition. It can also be read as a *chiral symmetry breaking*.

For simplicity, we will consider again only the lightest quarks: u, d, and s. In the QGP phase quarks already have mass gained at electroweak phase transition temperature scales, from Yukawa sector of MSM Lagrangian. But their mass is still very small, such that in ultrarelativistic aproximation it can be neglected. To get a sense of the numbers in question: from a mass comparable to electron mass (0.511 MeV), they reach through chiral symmetry breaking the value $\sim 1/3$ nucleon mass (940 MeV) [16]. Then arguably in QGP quarks obey the approximate symmetry $SU(3)_L + SU(3)_R$.

As the system approaches critical temperature T_c, the strength of the strong interaction between quarks increases such that quark-antiquark pairs form. After T_c the vacuum state contains such pairs, such that the vacuum expectation value of a pair becomes non-zero:

$$\langle \overline{\psi}_L \psi_R + \overline{\psi}_R \psi_L \rangle \neq 0. \tag{4.8}$$

Left and right fermions in a pair have opposite momenta and the total angular momentum of a pair is zero. Chiral symmetry breaking refers to this effect: the ground state of the system no longer obeys the chiral symmetry of the Lagrangian. The ground state is only invariant to fine tuned left and right rotations (in flavor space). Then the chiral symmetry breaking is abbreviated in the following expression:

$$SU(3)_L + SU(3)_R \to SU(3)_{L+R}. \tag{4.9}$$

Fermions moving in the non-zero expectation value $\langle \overline{\psi}\psi \rangle$ vacuum gain mass. The process can be intuitively summed in the following way: A right helicity quark in-

teracts with the condensate (4.8) and is annihilated by the right helicity antiquark. Then a left quark remains to move in vacuum with the same momentum. The observer just sees a particle which has changed its helicity, which means a particle with mass. The rate at which quarks change their helicities is proportional to (4.8). This process describes how quarks get *dynamical-generated mass* [16]. The chiral symmetry breaking has further consequences. Associated to each broken symmetry there is a massless Goldstone boson. In our *approximate* symmetry breaking (4.9), the associated bosons gain mass from the initial quark masses. It can be proved that pions are such associated particles, and their mass can be predicted accordingly (~ 140 MeV) [17].

As lattice simulations for the QCD phase transition yield one set of values, the two perspectives of seeing the phase transition must be complementary. It is not fully understood how deconfinement and chiral symmetry breaking describe the same phenomena. However some analogy between them can be drawn. Quarks particles bouncing from the bag surface reverse their momentum, but keep the same angular momentum. So they change their helicity at the surface. This process can be seen as helicity changing interaction with pairs in the bulk vacuum. So the bags can be conceived as bubbles of $\langle\overline{\psi}\psi\rangle = 0$ in a $\langle\overline{\psi}\psi\rangle \neq 0$ surrounding phase [16].

4.4 High Density QCD: The CFL Phase

On the QCD phase diagram, the universe as a whole follows the path of small baryon chemical potential μ and high temperatures. But in recent years the theorists interests was also captured by phase transitions happening at relatively small temperature and high μ. This limit is not encountered in the early universe, but there is hope to be realized in astrophysical objects of very high density, such as neutron stars.

Working in the limit $\mu \gg T$ made QCD more theoretically tractable and enabled construction of models that comprehensively predict the behavior of the system. The central argument explaining the simplification of QCD calculations revolves again around the idea of *asymptotic freedom*. At high densities or small distances the coupling between quarks becomes small, such that a perturbative treatment should become possible. But this is not entirely true, as perturbative expansions carried around the ground state, Fermi sphere, are plagued by infrared divergences [18]. This problem was eventually solved by invoking *color superconductivity*. In a movement reminiscent of condensed matter theory, it was found that quark matter at high μ can undergo transitions to superconductive phases in which a version of Meissner effect takes place, such that infrared divergences disappear with gluons gaining mass. Among these superconductive phases, we will focus here on the *color-flavor locking* (CFL) phase and the transition leading to it.

How does color superconductivity come into the QCD picture? At high densities of quarks, the system can be considered to form a degenerate Fermi gas. Even though we encounter typical temperatures of $O(10$ MeV$)$, they imply only small

fluctuations around the Fermi sphere (for example, in neutron stars $\mu \simeq 400 - 500$ MeV). Thus we can conclude that Fermi energy E_F is approximately equal to the baryon chemical potential μ. Further more, the strong interactions are weaker due to high μ. So, if interactions are for the moment neglected, this implies that adding a particle or a pair of particles to the system does not change the free energy F. $\Delta F = E - \mu N$, and adding a particle, $N = 1$, leads to $F = E_F - \mu \simeq 0$. Now, if we factor in the strong interaction, that means that the free energy will be diminished with the strength of that interaction. That further implies that pair of quarks are energetically favored to form at the Fermi surface, such that F is lowered. Thus the true ground state will be formed by condensates of quarks antisymmetric in color. This phenomena is similar to the one encountered in BCS theory, where the ground state is formed by condensates of electrons. Actually, in high μ QCD, we are in a better position than in ordinary BCS theory. There, electrons form pairs overcoming the Coulomb repulsion through phonon interactions. But this fact makes the pairs very sensitive to temperature increase. Quark pairings are in this respect much more robust as the strong force is naturally attractive and greater (even with the trend set by the running of the QCD coupling constant). So more energy is necessary to break the pairs. This in turn leads to higher energy gaps Δ ($\sim 10 - 100$ MeV [18]) and hence to superconductivity.

A further consequence of pairing quarks antisymmetric in color is that local color symmetry $SU(3)_c$ gets broken [19]. A similar process to Higgs mechanism takes place: the gauge bosons, which in this case are the gluons, get mass by the presence of a non-zero vacuum expectation value provided by quark pairs.

What is the form of the quark condensate? The prevalent models of QCD at high baryon chemical potential μ consider an idealized version of QCD in which only the three lightest quarks in our system: u, d and s play a role [18]. Still, there are more then one way to form these condensates, as quarks display flavor, color and spin degrees of freedom. In the following, we will consider the CFL phase which is dominant to the highest values of the baryon chemical potential μ. The argument for CFL is that it couples all the quarks, "leaving the maximal unbroken symmetry group" [18]. Thus all gluons gain mass and all infrared divergences are eluded. Also it leads to the highest energy gaps as the free energy is lowered the most (due to interactions among *all* three quarks). These features made the CFL phase the most attractive to the theorist and subsequently the best investigated.

The form of the CFL condensate reads [18]:

$$\langle \psi_{iL}^{a\alpha}(\mathbf{p}) \psi_{jL}^{b\beta}(-\mathbf{p}) \epsilon_{ab} \rangle = -\langle \psi_{iR}^{a\alpha}(\mathbf{p}) \psi_{jR}^{b\beta}(-\mathbf{p}) \epsilon_{ab} \rangle = \Delta(\mathbf{p^2}) \epsilon^{\alpha\beta A} \epsilon_{ijA}, \tag{4.10}$$

where (a, b) denote spinor indices, (i, j) flavor indices and (α, β) color indices, while Δ denotes the energy gap. The summed index A makes possible to write:

$$\epsilon^{\alpha\beta A} \epsilon_{ijA} = \delta_i^\alpha \delta_j^\beta - \delta_j^\alpha \delta_i^\beta. \tag{4.11}$$

This explains the name of the CFL phase. We see color indices coupled to flavor indices in a specific way. But QCD obeys the following local symmetries: $SU(3)_c \otimes$

$SU(3)_L \otimes SU(3)_R$ [19], where $SU(3)_{L,R}$ are flavor symmetries of the 3 quarks. By coupling flavor and color indices, the ground state is no longer invariant under independent color and flavor symmetries. Chiral symmetry is indirectly broken by the having both $SU(3)_L$ and $SU(3)_R$ locked to the color symmetry. Thus the system is invariant only under combined color and flavor transformation: this is CFL, *color-flavor locking*. In short, the symmetry breaking is illustrated here:

$$SU(3)_c \otimes SU(3)_L \otimes SU(3)_R \otimes U(1)_B \rightarrow SU(3)_{c+L+R} \otimes \mathbb{Z}_2. \tag{4.12}$$

$U(1)_B$ denotes the baryon number symmetry and it is broken to $\mathbb{Z}_2$ symmetry under which quark fields are multiplied by -1 [18].

By completely breaking the color symmetry, all gluons acquire the same mass [1]:

$$m_G^2 = \frac{g_s^2 \mu^2}{2\pi^2} + \frac{g_s^2 T^2}{2}, \tag{4.13}$$

and a version of Meissner effect for strong interactions takes place. But interestingly enough, there remains an unbroken $U(1)$ symmetry. Remember that at electroweak scale $SU(2)_L \otimes U(1)_Y$ is broken to electromagnetism $U(1)_Q$ such that W and Z bosons acquire a mass; but there is a combination of generators $t_3 + Y/2 = Q$ that annihilates the ground state, defining the unbroken $U(1)_Q$, such that electromagnetic forces mediated by photons remain long range. Similarly, in CFL, if we introduce the (up to now) neglected $U(1)_Q$ of electromagnetism in (4.12), there is a combination of generators that annihilate the ground state [18]:

$$\tilde{Q} = Q + \frac{1}{\sqrt{3}} T_8, \tag{4.14}$$

with T_8 a generator of the color group:

$$\begin{aligned} Q &= \text{diag}(\frac{2}{3}, -\frac{1}{3}, -\frac{1}{3}) \quad \text{in flavor } u, d, s \text{ space} \\ T_8 &= \frac{1}{\sqrt{2}} \text{diag}(-2, 1, 1) \quad \text{in color } r, g, b \text{ space} \end{aligned} \tag{4.15}$$

Thus we talk about a modified photon $\tilde{A}_\mu$ to which the superconductor is transparent and about an associated modified long range electromagnetic force. Regular light would be refracted inside the color superconducting as $\tilde{Q}$-light, and a $\tilde{Q}$-field, inside, would obey Maxwell equations.

Within the CFL phase, at chemical potential $\mu > 10^8$ MeV, perturbative calculation could be carried rigorously, such that from QCD Lagrangian gap energy was obtained [19]. Effective theories and renormalization group were devised to make the theory work at lower chemical potentials μ. Using initially renormalization group techniques near Fermi surface and assuming that CFL remains valid for μ on the order of neutron stars, the expression of the calculated gap energy reads [20]:

$$\Delta \simeq \frac{b\mu}{g_s^5} e^{-c/g_s} \qquad \text{with } c = \frac{3\pi^2}{\sqrt{2}} \tag{4.16}$$

with the estimate $b \simeq 512\pi^4 2^{-1/3}(2/3)^{5/2}$ [18]. Furthermore, from the gap equation, the critical temperature to CFL phase was found [19]:

$$T_c \simeq 0.57\Delta \simeq 50 \text{ MeV}. \tag{4.17}$$

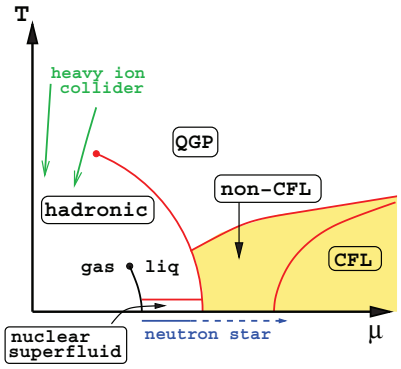

Figure 4.2: QCD phase diagram [19].

There are to this date no experiments to investigate the CFL phase (or the transition to it). The critical temperature T_c is far too low to be explored in heavy ion collisions. It is theorized that CFL could be realized in neutron stars, but it is not sure if $\mu \sim 400$ MeV is enough for CFL to form. Most likely nuclear matter or color superconducting phases different than CFL form most of a neutron star's core. Even assuming the presence of an inner core CFL phase, its signature would be highly elusive, as a color superconducting core would be essentially inert, with little influence on the parameters describing the behavior of the star [18]. Still some speculative experiments were proposed for detecting the CFL [18, 19]. As an example, we will be touching one of them. During a supernova event, a neutron star constitutes the remnant due to gravitational collapse of the core of exploding massive star. In a few seconds the stars cool from ~ 50 MeV to ~ 10MeV [16] by emitting neutrinos. If CFL is realized in the neutron star, the neutrinos pass without scattering from the superconducting core, as they have smaller energy than the gap Δ; otherwise they scatter from the core. Then it should be possible to detect a difference between supernovae in which a CFL neutron star is formed or not by noting the delay in emitted neutrinos. When scattering is involved, the main neutrino flux lasts 10-20 seconds, while, if CFL is realized, the flux should last much less.

4.5 Looking for the QGP

Lacking direct astrophysical data about the QCD phase transition, much effort was invested in recreating the quark-gluon plasma phase in laboratory conditions. The

avenue followed involves experiments with heavy ions (S, Pb or Au) in relativistic collisions. The first experiments were undertaken at Super Proton Synchrotron (SPS) at CERN and at Alternative Gradient Synchrotron (AGS) in Brookhaven using fixed target nuclei. Later on, starting in 2000, experiments begun at Relativistic Heavy Ion Collider (RHIC) in Brookhaven at much higher energies in CM and with better results. We will focus here on the RHIC experiments [21, 22]. The issue of weather QGP phase appears in such collisions will hopefully be settled at the LHC, with experiments at the ALICE detector.

In the RHIC experiments, gold nuclei were used in collision Au+Au, with 200 AGeV available in CM. The purpose was to create the conditions for deconfinement inside the initial fireball. The collision process is envisaged taking place in the following stages [16]. Relativistic gold nuclei crash together creating a fireball in which QGP phase is formed. As the fireball expands and cools, a transition to the hadronic phase takes place. At this point hadron composition is fixed and we talk about *chemical freeze-out*. Shortly after, within the expanding fireball, interactions rates among particles are insufficient to maintain thermal equilibrium, such that *thermal freeze-out* occurs. At this point the hadrons become free streaming and reach the detectors. Information about the conditions inside the initial fireball must be deduced from the last scattering surface at thermal freeze-out.

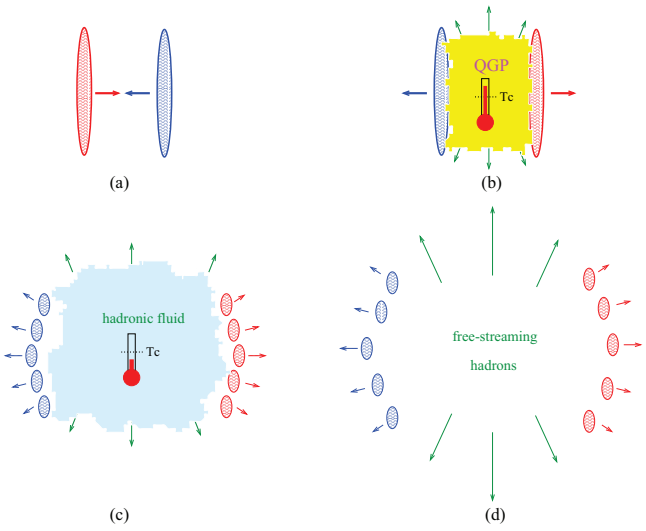

Figure 4.3: Stages in relativistic heavy-ion collisions [16].

Are these stages really describing the actual collision process? Are the conditions for deconfinement met? As the transition to QGP is predicted to take place at a critical temperature $T_c \simeq 175$ MeV, first condition is to attain enough energy during the collision process. With knowledge of the kinetic energy of the particles reaching detectors, it was possible, from an energy loss calculation, to predict the energy available in the small volume of the fireball [22]. The energy density ϵ pre-

dicted is $\epsilon \approx 5$ GeV/fm^2, which is 5 times the energy density required to reach te lattice calculated T_c [21].

The condition for the simple two phase transition model to apply is that chemical and thermodynamical equilibrium is attained in the system. This is not a trivial matter due to the highly violent nature of the collision process and due to the short lifetime t of the initial fireball, $t \approx 10$ fm/c [21]. Presence of chemical and thermodynamical equilibrium is supported by evidence obtained from considering ratios of detected particles. At T_c with a baryon chemical potential $\mu = 29$ MeV, these ratios are well described by statistical models that assume equilibrium [22]. The idea of thermodynamical equilibrium is also supported by the particle momentum spectra obtained at RHIC. It turns out that the flow of particles is well described by ideal hydrodynamical calculation assuming an ideal relativistic fluid flow (of the QGP type) in the center of the fireball, very early in its lifetime ($t \lesssim$ 1fm/c), and thus implying an early thermalization [21]. But as there is still work to be done investigating the sensitivity of the hydrodynamical calculations and predictions to the various parameters in the process, we cannot identify the QGP phase on this basis alone.

Even if the idea that conditions for QGP phase to form are met gets more and more experimental support, the next issue to be solved remains weather QGP is truly realized in the fireball. Here we will focus on two phenomena that seem to indicate the presence of the QGP state: *strangeness enhancement* and J/ψ *suppression*.

Strangeness enhancement refers to the fact that an unusual abundance of baryons containing the strange quark s, $\Lambda(uds), \Xi(ssd)$ and $\Omega(sss)$, was detected in the particle flow, at RHIC [16]. Explanation of this effect invokes the presence of QGP as a medium in which strange quarks are actually lighter due to restoration of chiral symmetry. Then higher densities of gluons lead to the opening of pair strange production channel by gluon fusion $gg \rightarrow s\bar{s}$. This creates the necessary conditions for having a population of *strange* baryons larger with more then a factor 10 in comparison to the one obtained at similar energy in pp and pA collisions.

J/ψ suppression refers to the relative scarcity of the J/ψ ($c\bar{c}$) meson in comparison with pA collisions at similar energies. The presence of QGP is again invoked to explain this effect. Inside the plasma the quark interaction is exponentially suppressed [16]:

$$V(r) = -\frac{C}{r} e^{-r/\lambda_D}, \tag{4.18}$$

where λ_D is the Debye screening length. As the equivalent Bohr radius for the charm quark c falls bellow λ_D, pairs of $c\bar{c}$ tend to dissociate. Thus, the numbers of J/ψ mesons are greatly reduced.

All these effects are indirect proof of the presence of the QGP phase. Future experiments to begin late in 2009 at LHC, carried at larger energies, will produce longer living fireballs at higher temperatures. The likeliness to produce the QGP phase is thus greatly increased. Also the above described signs of the QGP will

gain sharpness as higher energetic jets of particles will be easier to analyze, thus helping us map the contents of the fireball.

Chapter 5

Conclusions

We have shown that universe's evolution from electroweak to QCD phase transition can be considered a walk on the boulevard of broken symmetries:

$$SU(3)_c \otimes SU(2)_L \otimes U(1)_Y \xrightarrow{EWPT} SU(3)_c \otimes U(1)_{EM} \xrightarrow{QCDPT} U(1)_{EM}, \tag{5.1}$$

At critical temperature, breaking symmetries was directly related to how order parameters in these transitions gain non-zero expectation value. This led to changes in behavior of relevant forces, because their mediators become massive. In the particular case of QCD phase transition, the color group is broken only in the sense of confinement of quarks into hadrons. It was also possible to read the QCD phase transition as an approximate chiral symmetry breaking:

$$SU(3)_L \otimes SU(3)_R \xrightarrow{QCDPT} SU(3)_{L+R}, \tag{5.2}$$

where lightest quarks u, d and s were considered initially massless.

Within MSM, both transitions turned out to be crossovers, such that detectable remnants are not expected from them. The transitions phase diagrams were discussed and relevant critical temperatures were listed. In QCD case, the critical temperature was determined analytically within a simple phenomenological model. Supersymmetric extensions to MSM allowed electroweak phase transition to become first order and this was shown to potentially explain today's matter-antimatter asymmetry.

At high densities and low temperatures on the QCD phase diagram, we discovered the color-flavor locking phase. This was proved to be a color superconductive state in which a version of Meissner effect takes place: gluons become massive after the breaking of $SU(3)$ color symmetry group.

Using experimental arguments, quark-gluon plasma phase was found to be most likely realized in RHIC experiments. Further experimental data to bring complete consensus on the issue are expected from LHC's ALICE detector.

Bibliography

[1] T. Prokopec, Lecture notes for cosmology: The standard cosmological model, 2008, http://www.phys.uu.nl/ prokopec/2scm.pdf.

[2] A. Rajantie, (2003), hep-ph/0311262, Lectures given at COSLAB Workshop on Cosmological Phase Transitions and Topological Defects, Porto, Portugal, 22-24 May 2003.

[3] V. Mukhanov, *Physical Foundations of Cosmology* (Cambridge University Press, 2005).

[4] J. I. Kapusta and C. Gale, *Finite-Temperature Field Theory* (Cambridge University Press, 2006).

[5] S. Dawson, (2008), hep-ph/0812.2190.

[6] E. Laenen, Lecture notes on standard model, 2008.

[7] M. Laine, (2001), hep-ph/0111349.

[8] K. Kajantie, M. Laine, K. Rummukainen, and M. E. Shaposhnikov, Nucl. Phys. **B493**, 413 (1997), hep-lat/9612006.

[9] K. Rummukainen, M. Tsypin, K. Kajantie, M. Laine, and M. E. Shaposhnikov, Nucl. Phys. **B532**, 283 (1998), hep-lat/9805013.

[10] J. M. Cline, (2006), hep-ph/0609145, Lectures given at Les Houches Summer School - Session 86: Particle Physics and Cosmology: The Fabric of Spacetime, Les Houches, France, 31 Jul - 25 Aug 2006.

[11] M. Laine and K. Rummukainen, Nucl. Phys. **B535**, 423 (1998), hep-lat/9804019.

[12] J. M. Cline and G. D. Moore, Phys. Rev. Lett. **81**, 3315 (1998), hep-ph/9806354.

[13] A. Riotto, Theories of baryogenesis, in *Trieste 1998, High energy physics and cosmology*, pp. 326–436, 1998, hep-ph/9807454.

[14] Z. Fodor and S. D. Katz, JHEP **04**, 050 (2004), hep-lat/0402006.

[15] M. Le Bellac, *Thermal Field Theory* (Cambridge University Press, 1996).

[16] S. Hands, Contemp. Phys. **42**, 209 (2001), physics/0105022.

[17] M. E. Peskin and D. V. Schroeder, *An Introduction to Quantum Field Theory* (Perseus Books, 1995).

[18] K. Rajagopal and F. Wilczek, (2000), hep-ph/0011333.

[19] M. G. Alford, A. Schmitt, K. Rajagopal, and T. Schafer, Rev. Mod. Phys. **80**, 1455 (2008), hep-ph/0709.4635.

[20] D. T. Son, Phys. Rev. **D59**, 094019 (1999), hep-ph/9812287.

[21] BNL Report No. 73847, 2005 (unpublished), http://www.bnl.gov/bnlweb/pubaf/pr/docs/Hunting-the-QGP.pdf.

[22] T. Ludlam, Nucl. Phys. **A750**, 9 (2005).